Morphology of the Musculus Uvulae in Vivo Using MRI and 3D Modeling Among Adults with Normal Anatomy and Preliminary Comparisons to Cleft Palate Anatomy

Jamie L. Perry, PhD[1], **Joshua Y. Chen, BS**[2], **Katelyn J. Kotlarek, MS**[3], **Abigail Haenssler, MS**[4], **David P. Kuehn, PhD**[5], **Bradley P. Sutton, PhD**[6], **Thomas J. Sitzman, MD**[7], **Xiangming Fang, PhD**[8]

[1.]Jamie L. Perry, PhD. Associate Professor. Department of Communication Sciences and Disorders, East Carolina University

[2.]Joshua Y. Chen, BS. Medical Student. Brody School of Medicine, East Carolina University

[3.]Katelyn J. Kotlarek, MS. Doctoral Candidate. Department of Communication Sciences and Disorders, East Carolina University

[4.]Abigail E. Haenssler, MS. Doctoral Student. Department of Communication Sciences and Disorders, East Carolina University

[5.]Bradley P. Sutton, PhD. Professor. Department of Bioengineering, Beckman Institute for Advanced Science and Technology, University of Illinois at Urbana-Champaign

[6.]David P. Kuehn, PhD. Professor Emeritus. Department of Speech and Hearing Science, University of Illinois at Urbana-Champaign

[7.]Thomas J. Sitzman, MD. Plastic Surgeon. Division of Plastic Surgery, Phoenix Children's Hospital, Department of Surgery, Mayo Clinic College of Medicine

[8.]Xiangming Fang, PhD. Associate Professor. Department of Biostatistics, East Carolina University

Abstract

Purpose: To investigate the musculus uvulae morphology *in vivo* in adults with normal velopharyngeal anatomy and to examine sex and race effects on the muscle morphology. We also sought to provide a preliminary comparison of musculus uvulae morphology in adults with normal velopharyngeal anatomy to adults with repaired cleft palate.

Methods: 3D MRI data and Amira 5.5 Visualization Modeling software were used to evaluate the musculus uvulae in 70 participants without cleft palate and six participants with cleft palate. Muscle length, thickness, width, and volume were compared among participant groups.

Results: ANCOVA analysis did not yield statistically significant differences in musculus uvulae length, thickness, width, or volume by race or sex among participants without cleft palate when

Corresponding Author: Jamie L. Perry, PhD, Department of Communication Sciences and Disorders, 3310V College of Allied Health Sciences, Mail Stop 668, East Carolina University, Greenville, NC 27834 USA, Phone: (252) 744-6144, Fax: (252) 744-6109, perryja@ecu.edu.

the effect of body size was accounted for. Two-sample T-test revealed that the musculus uvulae in participants with repaired cleft palate is significantly shorter ($p = 0.008$, 13.6 mm vs. 16.1 mm) and has less volume ($p = 0.002$, 51 mm^3 vs. 98 mm^3) than participants without cleft palate.

Conclusion: In adults with normal velopharyngeal anatomy, the musculus uvulae is a cylindrical oblong-shaped muscle lying on the nasal surface of the soft palate, with its greatest bulk located just nasal to the levator veli palatini muscle sling. In subjects with repaired cleft palate, the musculus uvulae is substantially reduced in volume. This diminished muscle bulk located just at the point where the palate contacts the posterior pharyngeal wall may contribute to velopharyngeal insufficiency in children with repaired cleft palate.

Keywords

musculus uvulae; morphology; magnetic resonance imaging; three-dimensional reconstruction; sex; race; cleft palate

Introduction

The velum is an anatomically complex structure whose four distinct muscles interact to achieve velopharyngeal closure during speech production and swallowing. While the levator veli palatini is the primary palatal muscle responsible for speech production, the musculus uvulae also plays an important role (Pigott et al., 1969; Azzam and Kuehn, 1977; Kuehn et al., 1988; Huang et al., 1997; Perry, 2011; Sumida et al., 2014). Contraction of the musculus uvulae produces the dorsal convexity of the velum, adds stiffness to the velum, and extends the velum toward the posterior pharyngeal wall (Kuehn et al., 1988). Recent computational modeling of the musculus uvulae demonstrated that an absent or dysmorphic musculus uvulae resulted in an inability of the velopharyngeal mechanism to establish appropriate closure force (Inouye et al., 2016).

The musculus uvulae in the non-cleft population consists of either a single muscle bundle (unpaired) or a double (paired) muscle bundle with both bundles lying within the body of the velum (Azzam and Kuehn, 1977; Langdon and Klueber, 1978; Kuehn and Moon, 2005). Although the single bundle, similar to double bundle, arises from two aspects, the degree of fusion may differ between individuals with normal velopharyngeal anatomy. The musculus uvulae fibers lie along the midline of the velum and dorsal to the crossed and interconnected levator veli palatini muscle fibers (Azzam and Kuehn, 1977; Langdon and Klueber, 1978; Boorman and Sommerlad 1985; Kuehn and Moon, 2005; Landes et al., 2012). The musculus uvulae fibers originate at the palatal aponeurosis near the region of the levator veli palatini sling (Azzam and Kuehn, 1977) and continue along the nasal surface of the velum. The musculus uvulae fibers begin to diffuse and become less distinct near the posterior one third of the velum and sparingly extend into the uvula proper where there largely glandular nodules and an absence of muscle tissue (Azzam and Kuehn, 1977; Huang et al., 1997).

To date, studies of the musculus uvulae have included histology, dissection, electromyography (EMG), and computational modeling based on hypothetical prediction-based scenarios (Azzam and Kuehn, 1977; Langdon and Klueber, 1978; Boorman and Sommerlad 1985; Huang et al., 1997; Kuehn and Moon, 2005; Landes et al., 2012; Inouye et

al. 2016). Because of the relative inaccessibility of the velopharyngeal system during dissection and the ex vivo process involved in histology, these methods provide a limited understanding of muscle tissue morphology. Additionally, these methods are used on cadaveric material and may not be representative of living participants. To the best of our knowledge, no studies have characterized the morphology of the musculus uvulae *in vivo*. Additionally, no studies have examined if the musculus uvulae shape and/or size is controlled by factors of sex and race. Because previous research (Perry et al., 2016) demonstrated a significant sex and race effect on velar length, velar thickness, and levator veli palatini muscle measures, it is expected that the musculus uvulae may similarly be impacted by these internal variables.

To improve our limited knowledge on the morphology of the musculus uvulae *in vivo*, we aimed to describe qualitatively the musculus uvulae morphology among adults with normal velopharyngeal anatomy and to determine if its morphology was related to race or sex. We hypothesized that, similar to other velopharyngeal variables that are in close proximity to this muscle (e.g., levator veli palatini muscle, velar length, velar thickness), the musculus uvulae would vary based on sex and race. As a preliminary analysis, we also sought to explore the impact of palatal anomalies on the morphology of the musculus uvulae by comparing the musculus uvulae among adults with repaired cleft palate.

Methods

Participants

After obtaining approval from our local Institutional Review Board, we recruited adult participants with normal velopharyngeal anatomy and adult participants with a history of repaired cleft palate to participate in this study examining effect of sex and race on velopharyngeal structures (Perry et al., 2016). Written informed consent was obtained for all participants. Participants classified as having normal velopharyngeal anatomy had no history of cleft palate, craniofacial anomalies, syndromes, neurologic disorders, hearing disorder, or speech disorder, and all had a normal oral mechanism exam indicating no oral abnormalities. Participants with repaired cleft palate self-reported no history of syndromes or secondary palate surgeries (e.g., pharyngoplasty), and indicated normal hearing as an adult at the time of their involvement in the study.

Definitions of racial groups were aligned with those outlined by the National Institutes of Health (NIH, 2001) and include Asian, Black, and White. For the Asian race, only individuals of Japanese descent were selected to participate given the higher incidence in palatal clefting compared with Chinese, Filipinos, and Koreans (Natsume et al., 1988). Black individuals were classified as non-Hispanic in origin and living in the United States with ancestry from black racial groups of Africa. White individuals were of European descent and non-Hispanic. As an inclusionary criterion, all individuals self-reported the same ancestry among three generations with biological parents and all biological grandparents having the same race. No participant reported Hispanic origin.

Seventy adult participants aged 19–34 years of age (mean age = 22.4 years, standard deviation = 3.4 years) with normal velopharyngeal anatomy and six adults with repaired

cleft palate aged 19–66 years (mean age = 31.2 years, standard deviation = 18.1 years) agreed to participate in this study and completed the imaging protocol. In the normative group, there were 33 males and 37 females, and the race distribution consisted of 24 White, 20 Black, and 26 Asian participants. There were equal males and females in the group with repaired cleft palate, as well as five White and one Asian participant. Of the six adults with cleft palate, three had bilateral cleft lip and palate and three had cleft palate only. Primary cleft repair was performed in different hospitals, and specific details regarding the surgical procedures were not provided nor could be obtained across all participants with a history of cleft palate.

Magnetic Resonance Imaging

Participants were scanned in the supine position using a Siemens 3 Tesla Trio (Erlangen, Germany) MRI scanner with a 12-channel Siemens Trio head coil. Motion was minimized by using an elastic strap around the forehead and cushions positioned around the head. During image acquisition participants were instructed to breathe through their nose with their mouth closed. The velum was in a relaxed and lowered position. The imaging protocol has been described previously (Perry et al., 2013). In brief, a high resolution, T2-weighted turbo-spin-echo 3D anatomical scan called Sampling Perfection with Application optimized Contrasts using different flip angle Evolution (SPACE) was used to acquire a large field of view sagittal scan covering the oropharyngeal anatomy. Images were obtained with 0.8 mm isotropic resolution and an acquisition time of 4 minutes and 52 seconds.

Image Analyses

Participants were scanned in the supine position using a Siemens 3 Tesla Trio (Erlangen, Germany) MRI scanner with a 12-channel Siemens Trio head coil using a 3D imaging protocol described previously (Perry et al., 2013). Images were transferred into Amira 5 Visualization Volume Modeling software (Thermo Fisher Scientific, Waltham, MA, US). Using a free-handed paintbrush tool in Amira Segmentation Editor, fibers of the musculus uvulae were identified in successive slices in this plane. These were taken together to create a voxel set as described previously (Perry et al., 2013; Kotlarek et al., 2017; George et al., 2018).

Qualitative assessments of the musculus uvulae morphology was made by the primary and senior author through systemic review of the 3D reconstruction and visual comparison of sequential oblique coronal and sagittal images used during segmentation for all subjects. The second author also performed qualitative assessments using the same methods and the two authors compared findings. Qualitative comparisons were performed prior to collecting quantitative measures. Measurements, shown in Figure 1 including total muscle volume, muscle length (Fig. 1A), vertical (superior to inferior) thickness (Fig. 1B), and horizontal (lateral) width (Fig. 1C) were then made using length and volumetric tools in Amira. Velar length was measured on the mid-sagittal plane as the curvilinear length of the velum (Perry et al., 2016). Finally, velar thickness was measured on the mid-sagittal plane by measuring the velum at the velar knee noted as the insertion point of the levator veli palatini muscle.

Statistical Treatment

Statistical analysis was conducted using IBM SPSS 22 (IBM Corporation, Armonk, NY). Descriptive statistics were used to compare means and standard deviations between groups by race, sex, and for preliminary comparison of the non-cleft control participants to the six participants with repaired cleft palate. A two-way analysis of covariance (ANCOVA) using the general linear model procedure in SPSS 22 was used to test for sex and race variations among the four musculus uvulae measures. Height and weight were used as covariates to account for the effect of body size on the measures. This statistical approach allows for simultaneous testing for both sex and race effects on the muscle while controlling for overall body size. Levene's test was used to verify whether the equal variance assumption is true and the Shapiro-Wilk test assessed the normality assumption. The null hypotheses for these tests were that the variances can be assumed to be equal or the distribution can be assumed normal. Independent samples t-tests were used to compare differences in the musculus uvulae between the cleft and noncleft groups.

Results

Normal Musculus Uvulae Morphology

Due to the type of MRI sequence (T2 weighted), muscle tissue is observed as dark gray and fluid, connective tissue, and fat are light colored. Air or cavity spaces are noted by a very dark or black color. The musculus uvulae was identified as the dark-colored round muscular tissue dorsal to the levator sling. A lighter colored tissue (likely fat and connective tissue, Kuehn and Moon, 2005) surrounded the musculus uvulae, visibly separating it from the levator sling. The anterior end of the muscle was always flat, displaying the thinnest (vertical superior to inferior distance) area of the muscle and usually relatively wide (in the horizontal dimension). The muscle became gradually thicker until it was roughly cylindrical in the third quarter of its length. The muscle then became narrower (in the horizontal dimension) toward the posterior end of the muscle before becoming diffuse and ending before the tip of the uvula proper. The musculus uvulae was visibly convex along its length in three quarters (n = 53) of the participants, following the curve of the velum. In the remaining subjects it appeared flat (n = 10) or slightly concave (n = 7). In all cases, the muscle matched the curvature and form of the velum being either curvilinear or linear in the sagittal view. There appeared a clear delineation of the muscle into two separate muscle bundles in 4 participants with normal velopharyngeal anatomy. The paired appearance of the muscle was particularly evident in the anterior regions of the palate and was not visualized the entire length of the muscle. Specifically, in no subject was a paired muscle observed posterior to the levator sling.

Among adults with normal velopharyngeal anatomy, the length of the musculus uvulae was approximately half the total length of the velum (mean = 0.48 mm, standard deviation = 0.07 mm, range = 0.33–0.65 mm). The maximum thickness of the musculus uvulae typically corresponded to roughly one quarter of the maximum thickness of the velum (mean = 0.27 mm, standard deviation = 0.06 mm, range = 0.15–0.51 mm). The musculus uvulae always began posterior to the bony hard palate at the region of the palatal aponeurosis. The location of greatest thickness (in the vertical dimension) and cross-sectional area was consistently

within the area of the levator sling, toward the posterior portion of the musculus uvulae. The area of greatest width (in the horizontal dimension) was more variable, sometimes being located in a flat area nearer the anterior end and other times closer to the middle of the length of the muscle.

Data were normally distributed, as assessed by Shapiro-Wilk test ($p > .05$). There was homogeneity of variances, as assessed by Levene's test for equality of variances. Thus, we failed to reject the null hypotheses enabling the use of an ANCOVA model. Results indicated no statistically significant difference in adults with normal velopharyngeal anatomy was found among sex or race groups when the effect of body size was accounted for (see Tables 1–2, Figure 2). The mean muscle length was 16.07 mm (standard deviation = 2.02 mm), ranging from 12.04 – 23.82 mm across individuals. The mean muscle thickness (in the vertical dimension) was 2.92 mm (standard deviation = 0.58 mm), ranging from 2.00–3.31 mm across individuals. The mean muscle width was 4.50 mm (standard deviation = 0.92 mm), ranging from 2.48–7.11 mm across individuals. Mean muscle volume was 97.62 mm^3 (standard deviation = 28.94 mm^3), ranging from 47.2–168.9 mm^3 across individuals.

Comparison to Adults with Repaired Cleft Palate

The musculus uvulae in those with repaired cleft palate appeared to be less distinct with limited delineation from surrounding tissue, when compared to the control participants. The cross-sectional area of the musculus uvulae was grossly reduced in diameter (thickness) compared to non-cleft individuals. The muscle also appeared to be located closer to the levator sling showing a less prominent gap between the two muscles than in the non-cleft participants, though this may be in part due to a thinner velum in general. The muscle otherwise resembled its counterpart in non-cleft individuals. That is, it was flat at its origin in the palatal aponeurosis, had its greatest cross-sectional area in the middle, and narrowed toward its posterior end at the base of the uvula proper. Five of the six participants with repaired cleft palate displayed a convex nasal velar surface, and one displayed a concave surface.

Comparison of musculus uvulae morphology among adults with normal velopharyngeal anatomy and repaired cleft palate is presented in Table 3 and Figure 3. Subjects with repaired cleft palate had smaller musculus uvulae in every dimension. Muscle length was significantly shorter ($p = .008$) among participants with repaired cleft palate (mean = 13.65 mm, standard deviation = 1.51 mm, ranging from 11.85 – 15.63 mm) compared to those with normal velopharyngeal anatomy (mean = 16.07 mm, standard deviation = 2.02 mm). Muscle volume was also significantly smaller ($p = .002$) among participants with repaired cleft palate (mean = 51.08 mm^3, standard deviation = 21.84 mm^3, ranging from 18.50 – 83.70 mm^3) compared to participants with normal velopharyngeal anatomy (mean = 97.62 mm^3, standard deviation = 28.94 mm^3). Though not statistically significant, musculus uvulae thickness ($p = .176$) and width ($p = .102$) in individuals with repaired cleft palate demonstrated smaller mean values compared to adults with normal velopharyngeal anatomy.

Discussion

This study describes the morphology of the musculus uvulae *in vivo* as visualized by MRI in adults with and without repaired cleft palate. At rest, the muscle appears long, thin, cylindrical-shape with sheet-like flattening at its anterior and posterior edges. The musculus uvulae thickness averaged 2.9 mm and its volume averaged 97.6 mm^3 in normal adults. After adjusting for subject height and weight, the muscle dimensions were not associated with subject sex or race. In adults with repaired cleft palate, the musculus uvulae had a 50% smaller volume, averaging only 51.1 mm^3, and was significantly shorter than in subjects without cleft palate. These results provide new insights on the shape and volumetric contribution of the musculus uvulae to shape of the poster velum and to assist in velopharyngeal closure.

Our findings of *in vivo* musculus uvulae morphology are consistent with those from prior *ex vivo* reports of the muscle location, shape, and form. In line with prior anatomic cadaver dissections and histology studies, we found that in adults with normal velopharyngeal anatomy, the musculus uvulae originates from the palatal aponeurosis within the midline of the velum, courses dorsal to the levator veli palatini muscular sling, has its greatest thickness near the levator sling, becomes more diffuse near the posterior one third of the velum, and becomes indiscernible at the base of the uvula (Azzam and Kuehn, 1977; Langdon and Klueber, 1978; Huang et al., 1997; Kuehn and Moon, 2005). We also confirmed that in some individuals, the musculus uvulae consists of two paired muscles bundles rather than a single midline muscle (Azzam and Kuehn, 1977) and we provide new insight into this paired arrangement with our finding that this paired structure, when present, appears most prominent in the anterior half of the velum. These findings confirm and expand our knowledge of the musculus uvulae anatomy.

We also found that the musculus uvulae appears to be somewhat smaller *in vivo* compared to human cadavers. In a cadaveric study of seven specimens, Azzam and Kuehn (1977) reported a mean musculus uvulae muscle diameter of 5.9 mm and range of 4.8–8.3 mm. We observed a mean muscle width of 4.50 mm and range of 2.48–7.11 mm. These differences are also likely due to the combined macro and microscopic approaches used by Azzam and Kuehn (1977). Using a microscopic approach allows for greater visibility of the terminal ends of the muscle fibers as compared to only macro views obtained by MRI data. The resting tone of the muscle tissue among living subjects compared to cadaveric tissue likely also contributes to the variations observed (Martin et al., 2001). The present study is also drawn from a larger sample than prior cadaveric studies, so it may provide a more accurate assessment of the variability in the musculus uvulae across individuals. Lastly, differences by age may also be a factor as the mean age of participants in the present study was 22 years of age while those in the Azzam and Kuehn (1977) study were in the fifth or sixth decade of life.

In addition to describing the morphology of the musculus uvulae *in vivo*, this study contributes to the literature by providing normative musculus uvulae measures among a large and diverse sample. Prior to this study, direct assessments of the musculus uvulae in individuals with normal velopharyngeal anatomy have ranged from 2–19 participants

(Azzam and Kuehn, 1977; Langdon and Klueber, 1978; Boorman and Sommerlad, 1985; Kuehn and Moon, 2005; Landes et al., 2011; Landes et al., 2012). Based on our previous research findings that velar length, velar thickness, and levator veli palatini muscle morphology vary significantly by sex and race (Perry et al., 2016), in the present study we hypothesized sex and race would also be associated with musculus uvulae morphology. However, we found no association between musculus uvulae length, thickness, width, or volume and subject race or sex.

It is possible that velopharyngeal muscles shape and configuration are variable based on the type of velopharyngeal closure patterns. For example, individuals who have a coronal closure pattern, relying on greater velar contribution for velopharyngeal closure, may have a larger musculus uvulae when compared to individuals using a sagittal closure pattern (relying more on lateral pharyngeal wall motion). Because of the static nature of the MRI data used in the present study, involvement of the musculus uvulae in velopharyngeal closure could not be examined.

The final aim of this study was to provide a preliminary comparison of the musculus uvulae among adults with and without a history of cleft palate. Although conclusions about the musculus uvulae among those with cleft palate cannot be drawn given the small sample size, our results demonstrate a method of comparison and point to likely areas of differences that should be explored in future studies. Our results show that the musculus uvulae in participants with cleft palate appears shorter with overall smaller volume compared to non-cleft participants. Measures of thickness and width also tended to be smaller, though this difference was not statistically significant. Caution should be taken in considering these findings, given the limited sample of only six adults with repair cleft and limited information on each participant's surgical history. Because surgical history was not able to be obtained among the adult participants with repaired cleft palate, comparison of muscle configuration based on surgery type cannot be performed. The observations from the present study agree with prior studies suggesting that the musculus uvulae is preserved to some degree in those with repaired cleft palate (Fara and Dvorak, 1970; Calnan, 1954).

Inouye et al. (2016) recently evaluated the contribution of the musculus uvulae to velopharyngeal closure using a computational model that simulates multiple scenarios of muscle abnormalities. The authors observed that with a 100% activation level of the musculus uvulae with low levels of levator veli palatini activation, the musculus uvulae had the capacity to preserve normal velopharyngeal closure. This finding supports the role of an active musculus uvulae in individuals with cleft palate, who often have hypoplastic and/or dysmorphic levator veli palatini muscle bundles (Ha et al., 2007; Kotlarek et al., 2017; Perry et al., 2018). However, when the bulk and contraction of the musculus uvulae was removed in this simulation, incomplete velopharyngeal closure was observed. These findings highlight the importance of the space-occupying function of the musculus uvulae. They also suggest that in subjects with an absent or hypoplastic musculus uvulae, surgical augmentation of the velum in the position of the musculus uvulae might create a more favorable convexity to the nasal velar surface and aid velopharyngeal closure. Future research should examine the effect of varied surgical techniques that involve using fat and/or muscle to increase the velar midline, such as overlapping levator muscle fibers (Woo et al.,

2014; Nguyen et al., 2015), buccal fat pad graft (Kim, 2001; Pinto and Pegoraro-Krook, 2007; Pappachan and Vasant, 2008; Levi et al., 2009; Yamaguchi et al., 2016), and bilateral buccal flap (Mann and Fisher, 1997; Mann et al., 2011). Although it is possible these techniques contribute to the role of the musculus uvulae as a space occupying muscle (particularly in a state when the muscle is hypoplastic), muscle imaging has yet to confirm these speculations.

This study has several limitations that must be noted. First, the sample may not have been sufficiently large to detect an interaction of both sex and race with musculus uvulae morphology. Second, the sample of six adults with repaired cleft palate is small and may be biased by unmeasured factors such as cleft palate type or method of cleft palate repair; additional research with a larger sample of subjects with repaired cleft palate is needed to address this question. Additionally, reliability was not assessed for qualitative measures. Finally, this study addresses only static muscle morphology at rest. Dynamic assessment of the muscle was not performed, so we cannot comment on morphology of the contracted musculus uvulae *in vivo*. Future research should involve muscle imaging and dynamic assessment tools, while also considering surgical techniques when investigating the impact of the musculus uvulae in individuals with repaired cleft palate.

Conclusion

The current study provides new insights on the morphology of the musculus uvulae using MRI scans obtained in a large and diverse sample of adults with normal velopharyngeal anatomy. Our results show that the musculus uvulae contributes substantial bulk to the velum, particularly at the point of palatal closure with the posterior pharyngeal wall. A comparison of control subjects to six patients with repaired cleft palate found that the musculus uvulae was significantly shorter and approximately 50% less voluminous in participants with repaired cleft palate. Future research is needed to understand the impact of the musculus uvulae on velopharyngeal function, particularly in the presence of dysmorphic anatomy such as cleft palate.

Financial Disclosure Statement:

References

Azzam N, Kuehn DP. The morphology of musculus uvulae. Cleft Palate J. 1977;14(1):78–87. [PubMed: 264280]

Boorman JG, Sommerlad BC. Musculus uvulae and levator palati: Their anatomical and functional relationship in velopharyngeal closure. Br J Plast Surg. 1985;38(3):333–338. [PubMed: 4016419]

George TN, Kotlarek KJ, Kuehn DP, Sutton BP, Perry JL. Differences in the tensor veli palatini between adults with and without cleft palate using high-resolution 3-dimensional magnetic resonance imaging. Cleft Palate Craniofac J. 2018;55(5):697–705. [PubMed: 29360409]

Ha S, Kuehn DP, Cohen M, Alperin N. Magnetic resonance imaging of the levator veli palatini muscle in speakers with repaired cleft palate. Cleft Palate Craniofac J. 2007;44(5):494–505. [PubMed: 17760495]

Huang MH, Lee ST, Rajendran K. A fresh cadaveric study of the paratubal muscles: Implications for eustachian tube function in cleft palate. Plast Reconstr Surg. 1997;100(4):833–842. [PubMed: 9290650]

Inouye JM, Lin KY, Perry JL, Blemker SS. Contributions of the musculus uvulae to velopharyngeal closure quantified with a 3D multi-muscle computational model. Ann Plast Surg. 2016;77(Suppl 1): 70–75.

Kim Y The use of a pedicled buccal fat pad graft for bone coverage in primary palatorrhaphy: A case report. J Oral Maxillofac Surg. 2001;59:1499–1501. [PubMed: 11732045]

Kotlarek KJ, Perry JL, Fang X. Morphology of the levator veli palatini muscle in adults with repaired cleft palate. J Craniofac Surg. 2017;28(3):833–837. [PubMed: 28060090]

Kuehn DP, Folkins JW, Linville RN. An electromyographic study of the musculus uvulae. Cleft Palate J. 1988;25(4):348–355. [PubMed: 3203466]

Kuehn DP, Moon JB. Histologic study of intravelar structures in normal human adult specimens. Cleft Palate Craniofac J. 2005;42(5):481–489. [PubMed: 16149828]

Landes CA, Weichert F, Steinbauer T, Schröder A, Walczak L, Fritsch H, Wagner M. New details on the clefted uvular muscle: Analyzing its role at histological scale by model-based deformation analyses. Cleft Palate Craniofac J. 2012;49(1):51–59. [PubMed: 21812575]

Landes CA, Weichert F, Steinbauer T, Walczak L, Hasenfus A, Veith C, Schröder A, Fritsch H, Theegarten D, Wagner M. Histology and function: Analyzing the uvular muscle. Cleft Palate Craniofac J. 2011;48(6):639–645. [PubMed: 20815710]

Langdon HL, Klueber K. The longitudinal fibromuscular component of the soft palate in the fifteen-week human fetus: Musculus uvulae and palatine raphe. Cleft Palate J. 1978;15(4):337–348. [PubMed: 281277]

Levi B, Kasten SJ, Buchman SR. Utilization of the buccal fat pad flap for congenital cleft palate repair. Plast Reconstr Surg. 2009;123(3):1018–1021. [PubMed: 19319069]

Mann RJ, Fisher DM. Bilateral buccal flaps with double opposing Z-plasty for wider palatal clefts. Plast Reconstr Surg. 1997;100(5):1139–1143. [PubMed: 9326774]

Mann RJ, Neaman KC, Armstrong SD, Ebner B, Bajnraugh R, Naum S. The double-opposing buccal flap procedure for palatal lengthening. Plast Reconstr Surg. 2011;127(6):2413–2418. [PubMed: 21617473]

Martin DC, Medri MK, Chow RS, Oxorn V, Leekam RN, Agur AM, McKee NH. Comparing human skeletal muscle architectural parameters of cadavers with in vivo ultrasonographic measurements. J Anat. 2001;199(4):429–434. [PubMed: 11693303]

Natsume N, Suzuki T, Kawai T. The prevalence of cleft lip and palate in Japanese. Br J Oral Maxillofac Surg. 1988;26:232–236. [PubMed: 3165019]

Nguyen DC, Patel KB, Skolnick GB, Skladman R, Grames LM, Stahl MB, Marsh JL, Woo AS. Progressive tightening of the levator veli palatini muscle improves velopharyngeal dysfunction in early outcomes of primary palatoplasty. Plast Reconstr Surg. 2015;136(1):134–141.

Pappachan B, Vasant R. Application of bilateral pedicled buccal fat pad in wide primary cleft palate. Br J Oral Maxillofac Surg, 2008;46:310–312. [PubMed: 17640783]

Perry JL. Anatomy and physiology of the velopharyngeal mechanism. Semin Speech Lang. 2011;32(2):83–92. [PubMed: 21948636]

Perry JL, Kotlarek KJ, Sutton BP, Kuehn DP, Jaskolka M, Fang X, Point SW, Rauccio F. Variations in velopharyngeal structure in adults with repaired cleft palate. Cleft Palate Craniofac J. 2018 [Epub ahead of print].

Perry JL, Kuehn DP, Sutton BP. Morphology of the levator veli palatini muscle using magnetic resonance imaging. Cleft Palate Craniofac J. 2013;50(1):64–75. [PubMed: 22023112]

Perry JL, Kuehn DP, Sutton BP, Gamage JK, Fang X. Anthropometric analysis of the velopharynx and related craniometric dimensions in three adult populations using MRI. Cleft Palate Craniofac J, 2016;53(1):e1–e13. [PubMed: 25525327]

Author Manuscript

Author Manuscript

Author Manuscript

Author Manuscript

Pigott RW, Bensen JF, White FD. Nasendoscopy in the diagnosis of velopharyngeal incompetence. Plast Reconstr Surg. 1969;43(2):141–147. [PubMed: 5765920]

Pinto JH, da Silva Dalben G, Pegoraro-Krook MI. Speech intelligibility in patients with cleft lip and palate after placement of speech prosthesis. Cleft Palate Craniofac J. 2007;44(6):635–641. [PubMed: 18177184]

Sumida K, Kashiwaya G, Seki S, Masui T, Ando Y, Yamashita K, Kitamura S. Anatomical status of the human musculus uvulae and its function implactions. Clin Anat. 2014;27(7):1009–1015. [PubMed: 25044008]

Woo AS, Skolnick GB, Sachanandani NS, Grames LM. Evaluation of two palate repair techniques for the surgical management of velopharyngeal insufficiency. Plast Reconstr Surg. 2014;134(4):588e–596e. [PubMed: 25357021]

Yamaguchi K, Lonic D, Lee C, Yun C, Lo L. Modified furlow palatoplasty using small double-opposing Z-plasty: Surgical technique and outcome. Plast Reconstr Surg. 2016;137(6):1825–1831. [PubMed: 27219237]
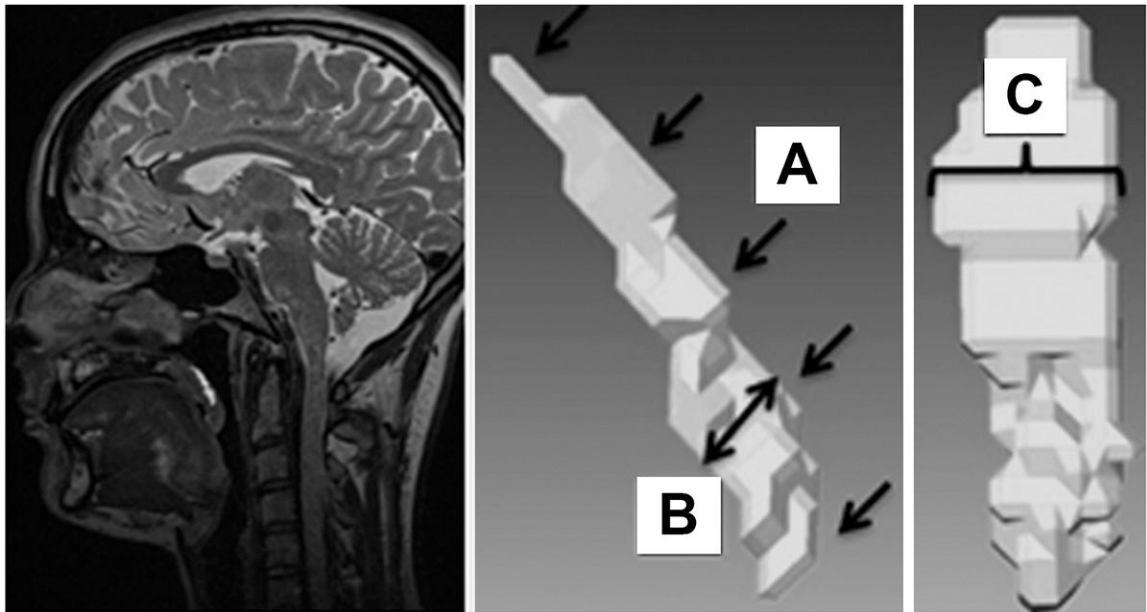
Figure 1.
Display of measurements taken on 3D reconstruction of musculus uvulae obtained from MRI data. The sagittal view demonstrates (A) length of musculus uvulae (indicated by multiple arrows along muscle contour) and (B) thickness of musculus uvulae (indicated by double-headed arrow) measured at the greatest thickness. The oblique coronal/axial view shows (C) horizontal width of musculus uvulae (indicated by the bracket) measured at the thickness width.
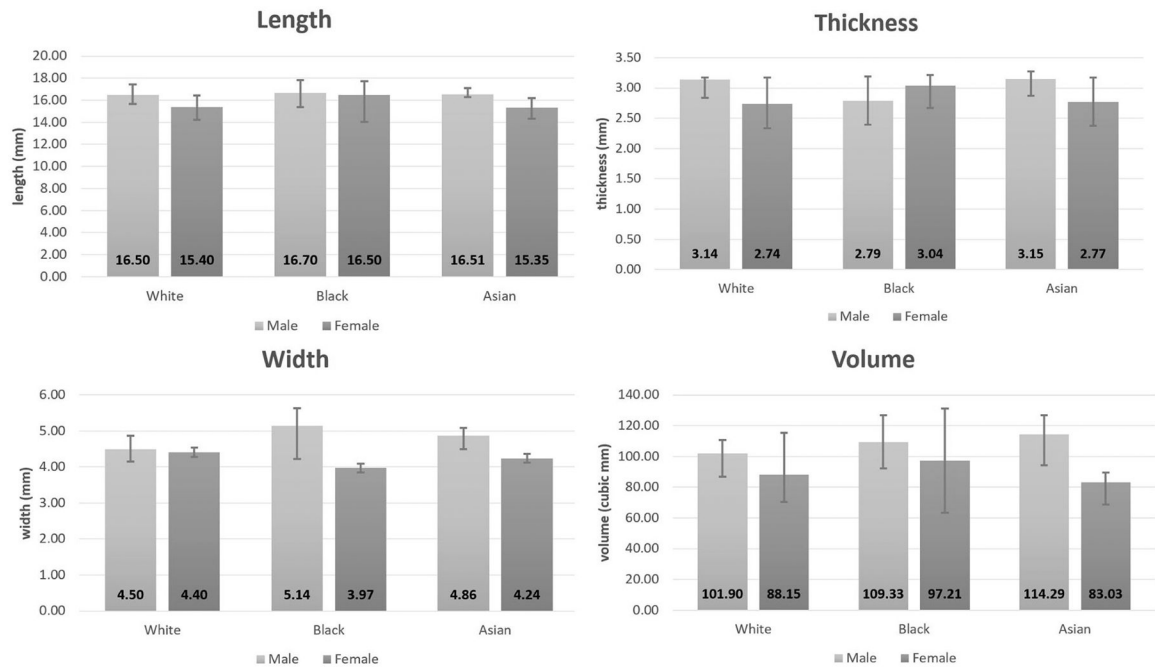
Figure 2.

Comparisons of musculus uvulae length (a), thickness (b), width (c), and volume (d) among sex and race groups in adults with normal velopharyngeal anatomy. Height of the bars represents mean values for each respective measure, and the error bars represent interquartile range.
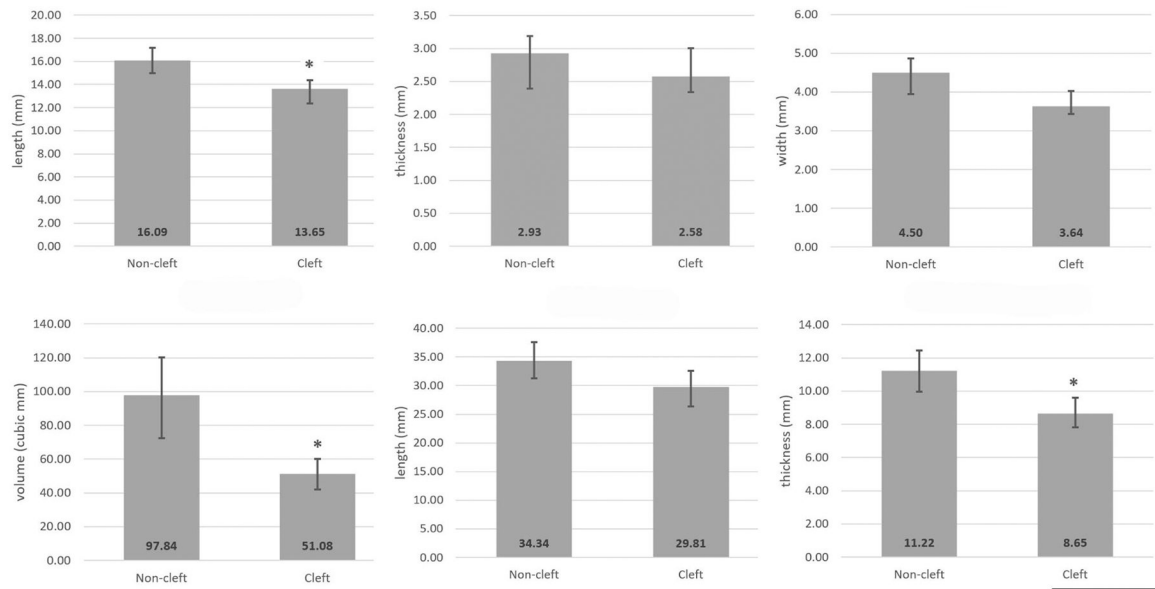
Figure 3.
Comparisons of musculus uvulae length (a), thickness (B), width (c), and volume (d) between participants with normal velopharyngeal anatomy and participants with repaired cleft palate, as well as comparisons of velum length (e) and velum thickness (f) as described in Perry et al. (2016). An asterisk (*) indicate statistically significant differences with $p < 0.01$.

Table 1.

Musculus uvulae measurements across groups by race, sex, and compared to the cleft palate group. Measures are reported in mm and mm^3 for volume.

		length		thickness		width		volume	
		mean	s. d.	mean	s. d.	mean	s. d.	mean	s. d.
White	*male* (n=12)	16.50	1.41	3.14	0.82	4.50	0.68	101.90	26.02
	female (n=12)	15.40	1.75	2.75	0.42	4.40	0.68	88.15	26.63
	combined (n=24)	15.95	1.65	2.94	0.67	4.45	0.67	95.03	26.69
Black	*male* (n=10)	16.70	2.65	2.79	0.50	5.14	0.56	109.33	25.58
	female (n=10)	16.50	3.25	3.04	0.48	3.97	1.23	97.21	40.06
	combined (n=20)	16.60	2.89	2.94	0.50	4.56	1.11	103.27	33.30
Asian	*male* (n=11)	16.51	1.40	3.15	0.66	4.86	1.16	114.29	22.01
	female (n=15)	15.34	1.44	2.75	0.46	4.23	0.82	82.25	25.02
	combined (n=26)	15.82	1.51	2.91	0.57	4.49	1.00	95.30	18.37
combined	*male* (n=33)	16.56	1.81	3.04	0.68	4.81	0.86	108.28	24.42
	female (n=37)	15.66	2.14	2.82	0.46	4.22	0.90	88.05	29.87
	combined (n=70)	16.07	2.02	2.92	0.58	4.50	0.92	97.62	28.94
cleft palate (n=6)		13.65	1.51	2.58	0.54	3.64	1.05	51.08	21.84

Table 2.

ANCOVA Results for participants without cleft palate

Source	Dependent variable	SS	df	MS	F	Significance
Sex						
	MU length	2.587	1	2.587	0.641	0.426
	MU thickness	0.601	1	0.601	1.708	0.196
	MU width	1.591	1	1.591	1.900	0.173
	MU volume	217.463	1	217.463	0.296	0.588
	Velar length	35.086	1	35.086	2.704	0.105
	Velar thickness	15.925	1	15.925	7.149	0.010
Ethnicity						
	MU length	3.364	2	1.682	0.417	0.661
	MU thickness	0.036	2	0.018	0.051	0.950
	MU width	0.303	2	0.151	0.181	0.835
	MU volume	1124.568	2	562.284	0.765	0.470
	Velar length	68.026	2	34.013	2.621	0.081
	Velar thickness	11.038	2	5.519	2.478	0.092
Weight						
	MU length	11.079	1	11.079	2.745	0.103
	MU thickness	0.014	1	0.014	0.040	0.842
	MU width	0.066	1	0.066	0.079	0.780
	MU volume	1175.843	1	1175.843	1.599	0.211
	Velar length	68.000	1	68.000	5.240	0.025
	Velar thickness	0.932	1	0.932	0.419	0.520
Height						
	MU length	0.990	1	0.990	0.245	0.622
	MU thickness	0.102	1	0.102	0.290	0.592
	MU width	0.151	1	0.151	0.181	0.672
	MU volume	704.981	1	704.981	0.959	0.331
	Velar length	1.008	1	1.008	0.078	0.781
	Velar thickness	0.439	1	0.439	0.197	0.659

Table 3.

T-test for equality of means between participants with and without repaired cleft palate.

	t	df	Mean difference	Significance	Std error difference
MU length	3.699	6.688	2.448	0.008	0.662
MU thickness	1.532	6.053	0.351	0.176	0.229
MU width	1.951	5.691	0.865	0.102	0.443
MU volume	4.885	6.632	46.762	0.002	9.573
Velar length	1.890	5.523	4.505	0.112	2.384
MU/velar length	0.666	5.579	0.023	0.532	0.035
Velar thickness	4.428	6.415	2.557	0.004	0.577
MU/velar thickness	−0.928	5.364	−0.034	0.393	0.037